CMX Journal Club: Coherent quantum phase slips and the development of the CQUID

Spencer Tomarken

August 10, 2018

References

Coherent quantum phase slips: *Nature* **484**, 355 (2012)
CQUID: *Nature Physics* **14**, 590 (2018)

Context

This set of notes represents an expansion of a CMX journal club chalk talk I presented on August 10, 2018. In the interest of time I skipped many derivations or took motivated shortcuts at the blackboard. Here I have included the extended calculations that were necessary for me to feel comfortable with the material as well as an expanded discussion whenever possible. These notes will be available for download at `http://cmx-jc.mit.edu/previous-talks`.

Introductory Remarks

The papers I chose to discuss today concern the physical effect of a "phase slip" in a superconducting nanowire. I will motivate today the fact that a suitable phase slip nanowire can be thought of as the electromagnetic dual to a Josephson junction (this will be unpacked in a bit). The first paper, which will be the main focus of this talk, demonstrated the existence of coherent quantum phase slips using microwave spectroscopy. The second paper, which I will not have time to discuss in detail but will offer brief commentary at the end, takes the next logical leap by creating a new circuit called a Charge QUantum Interference Device (CQUID) which is the dual to the more well known SQUID.

In light of these themes, perhaps it's best to begin by acknowledging that the field of electromagnetism has many conjugate pairs. After all, we don't call it simply "electricity" or "magnetism". Some of us are even too uncomfortable with the term "electricity and magnetism" so we coined a new term "electromagnetism" to emphasize the deep interrelationship between electric and magnetic phenomena. We have electric and magnetic fields, capacitors and inductors, scalar

and vector potentials, etc. Unfortunately, magnetic "charge" or magnetic monopoles do not exist, but in the context of a circuit it turns out that a suitably defined magnetic flux is the conjugate to electric charge. This can be motivated by noting that the elementary magnetic field source is an infinitesimal Ampèrian current-carrying loop.

In order to come up with some basic intuition as to why a Josephson junction (JJ) is a conjugate to the quantum phase slip (QPS) site, consider a cartoon picture of a JJ as drawn in Fig. 1. One type of JJ consists of a local disruption of a superconducting wire by an insulating barrier. Due to the local overlap of the superconducting condensate wave functions on either side of the insulating barrier, Cooper pairs can be coherently shuttled across the junction in a disipationless process. When the current across the junction exceeds a maximum threshold, the JJ become dissipative. I will explain shortly that dissipation in a JJ corresponds to jumps in the phase across the junction in factors of 2π. While this occurs, the total change in flux across the element is one flux quantum ϕ_0. We can imagine flux moving along the insulating barrier (we could picture connecting the junction to a closed circuit to consider the flux through a closed loop) during such a process.

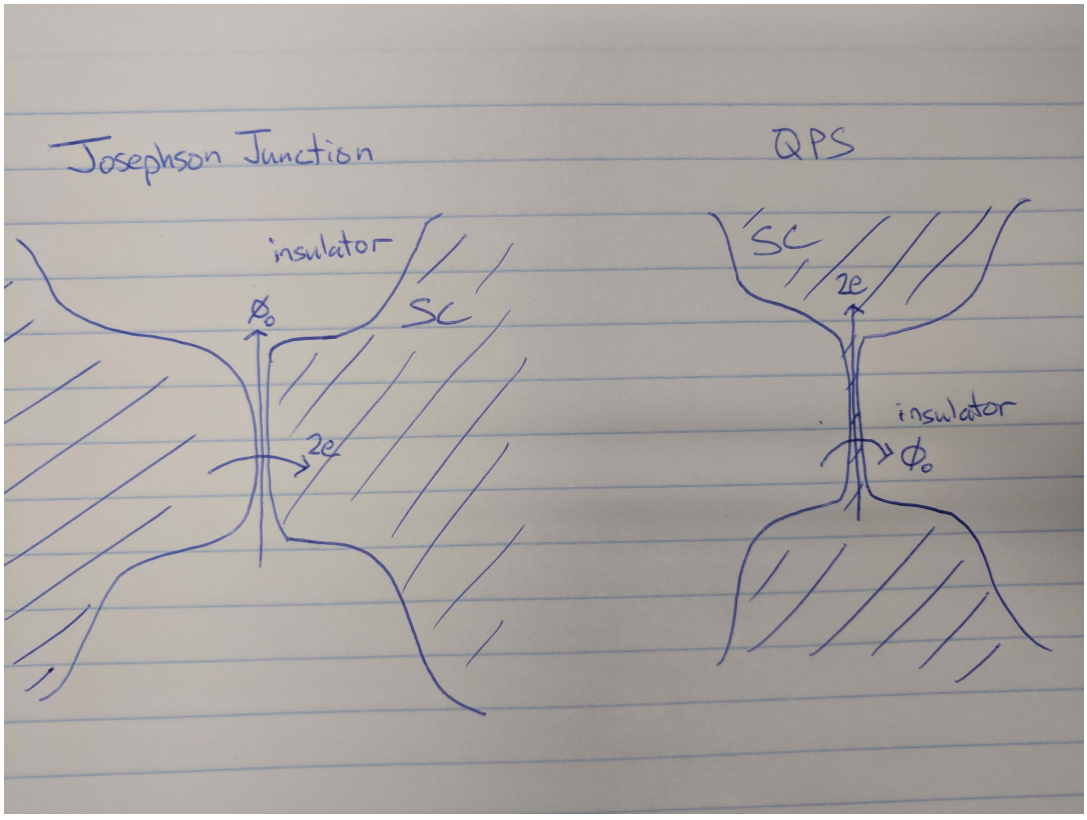

Figure 1: (Left) Cartoon of a Josephson junction. The two thick wires (shaded regions) come into close proximity and are separated by an insulating barrier. $2e$ charge tunnels across a barrier while flux passes through the junction. (Right) "Dual" schematic consisting of a nanowire segment carrying charge down the wire while flux tunnels across the junction.

In a very naïve way, we can run with this concept of duality and simply swap out all conju-

gate pairs. We will exchange superconductor $\leftrightarrow$ insulator and flux $\leftrightarrow$ Cooper pairs. If we rotate our perspective 90 degrees we now have two thick superconducting wires connected by a thin superconducting wire as shown in Fig. 1. Note that we assume here that the thin nanowire is not a "Dayem bridge" type JJ. The order parameter of the superconductor is robust throughout the entire wire and is capable of carrying supercurrent without Cooper pair tunneling. In this picture, we have Cooper pairs that are passing along the thin wire and we have a flux quantum that we can picture tunneling or hopping over the wire. Despite being simplistic, this cartoon serves to motivate the duality between JJs and phase slip sites. We will now build up a more detailed treatment.

Dissipation in the Josephson junction

It turns out that quantum phase slips are quite a bit more challenging to describe precisely than the more well-known JJ. The elementary relationships of the JJ can be derived with a few lines of algebra (e.g. Kittel, Tinkham). To properly treat phase slips requires quite a bit more machinery. We will not have time to cover these details in a one hour talk. Instead, we will cover the role of phase and flux in the context of dissipation in a JJ and then explore phase slip sites using some of the formalism we develop for the JJ.

The two fundamental equations we will be using to describe a Josephson junction are:

$$I = I_c \sin\gamma$$
$$\frac{d\gamma}{dt} = \frac{2eV}{\hbar}$$

where γ represents the phase difference between the two superconductors across the junction and I_c is the critical current of the junction. The critical current is given by $I_c = \frac{\pi\Delta}{2R_n e}$ at $T = 0$ where R_n is the normal state resistance of the junction and Δ the superconducting gap at $T = 0$. The critical current is dependent on both the superconductor material as well the junction geometry. It is roughly a measure of how many Cooper pair modes can be sustained across the junction simultaneously.

The equation $I = I_c \sin\gamma$ is, in fact, only applicable in a particular limit: $I < I_c$. When I exceeds I_c, γ is a function of time and we now have a finite voltage across the junction. We will need a more sophisticated model to proceed. If we think about the JJ in detail, we might guess a few useful additions. The JJ consists of two pieces of metal extremely close together – there will likely be a relevant capacitance C across the junction. Similarly, when we exceed the critical current we must start sending charge across in single electrons which must experience a resistive dissipation R (which is strongly temperature dependent). We can imagine modeling the JJ as one pure JJ element described by the two essential equations above along with a capacitor C and resistor R in parallel, effectively shunting the junction as depicted in Fig. 2. This is known as the resistively

and capacitively shunted junction (RCSJ) model. If we apply a current bias I across the junction we can sum up the current from each branch:

$$I = \Sigma_i I_i = I_c \sin\gamma + \frac{V}{R} + C\frac{dV}{dt}.$$

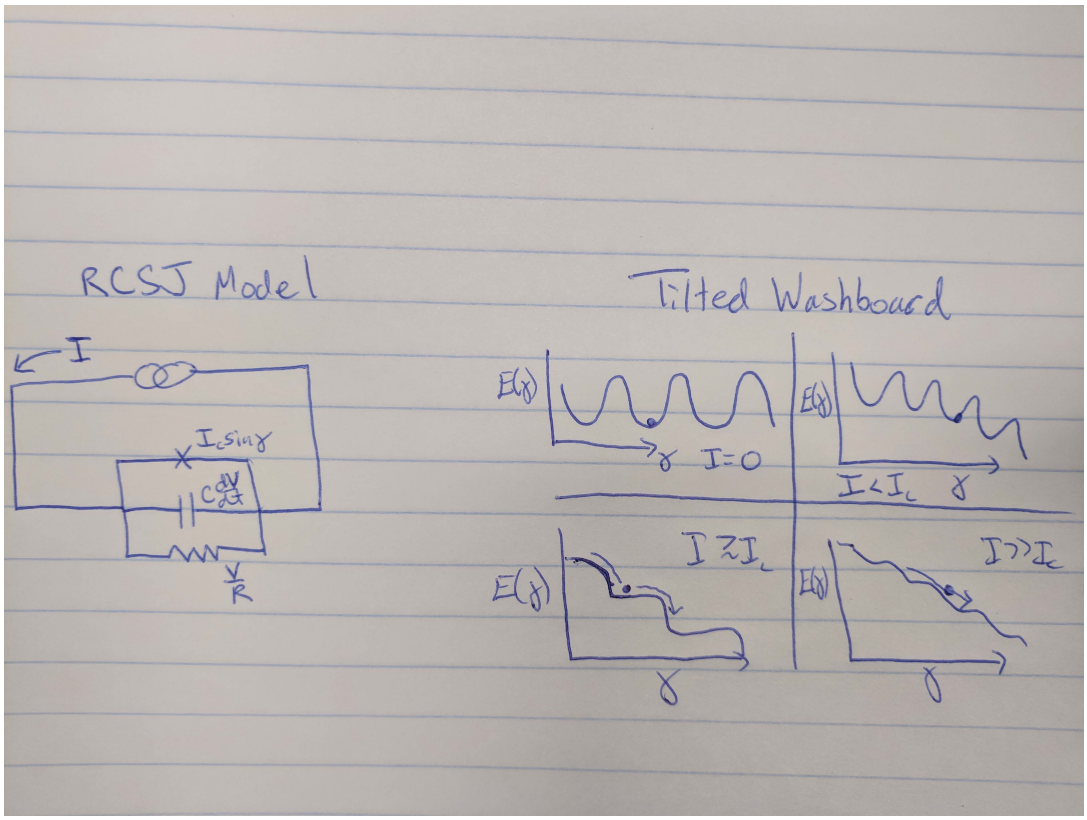

Figure 2: (Left) Resistively and capacitively shunted junction model: we picture the JJ as consisting of an ideal Josephson element in parallel with a capacitor and resistor. (Right) In the tilted washboard picture, we can treat the phase γ as a dynamical variable in a potential that obeys a deterministic, classical equation of motion.

Because we have a linear relationship $d\gamma/dt \sim V$, we can swap out dependence of V for dependence on γ at the mere cost of a time-derivative and some dimensionful factors. We wind up with the following relationship:

$$\frac{d^2\gamma}{d\tau^2} + \frac{1}{Q}\frac{d\gamma}{d\tau} + \sin\gamma = \frac{I}{I_c}.$$

It is not crucial for this lecture, but for completeness the substitutions we have made are the fol-

lowing:

$$\tau = \omega_p t$$
$$\omega_p = \sqrt{\frac{2eI_c}{\hbar C}}$$
$$Q = \omega_p RC.$$

Inspection of the second order differential equation reveals that it looks awfully like an equation of motion for a particle of coordinate γ containing an inertial term, a friction term, and a set of applied forces. In the context of the RCSJ parameters, the inertial mass $m \sim C$ and the friction term $\beta \sim \frac{1}{R}$. If we integrate the forces to calculate the potential experienced by the phase we find a very important equation:

$$U(\gamma) = -E_J \cos\gamma - \frac{\hbar I}{2e}\gamma = -E_J\left(\cos\gamma + \frac{I}{I_c}\gamma\right)$$

where the Josephson energy $E_J = \frac{\hbar I_c}{2e}$. We can utilize this potential profile to imagine the dynamics of the phase γ as we manipulate the current bias I as well as consider different limits of the parameters I_c, C, R. Let's start with a simple case: $I = 0$. We are not flowing current through the device and the potential is simply a negative cosine function (see Fig. 2). The phase of the junction is a minimum whenever $\gamma = 2\pi n$ for $n \in \mathbb{Z}$. Importantly, this solution is stationary in time. The system does not evolve. If we now imagine slowly increasing I such that $I < I_c$ our cosine shape begins to tilt downward to the right due to the linear term in the potential. Another name for the RCSJ model is the appropriately titled "tilted washboard" model. As long as $I < I_c$ we can always find a suitable local minimum given by $\gamma = \sin^{-1}(I/Ic)$. Physically, we can imagine our potential like a track and our phase a marble running along its profile. If we slowly tilt our potential down, the marble will simply shift to the right from its previous $I = 0$ equilibrium as it finds a new local minimum. Importantly all of these solutions are stationary in time. Something special happens when we exceed I_c. We no longer have local minima and the phase simply "runs" down the track.

In order to extract some insight we can take the useful limit that C is small. This corresponds to removing the second-derivative term in the equation of motion. Because C represents the inertia, this corresponds to an "infinite friction" situation in which the speed of γ is always proportional to the local slope of the track. Under this condition the equation of motion reduces to:

$$\frac{d\gamma}{d\tau} = \frac{2eI_cR}{\hbar}\left(\frac{I}{I_c} - \sin\gamma\right).$$

Let's consider when I just barely exceeds I_c so that $\frac{I}{I_c} \sim 1$. In this situation, the potential profile looks like a staircase. The previous minimum of the $\cos\gamma$ term have been just flattened out into shoulders by the linear current bias term. Because the rate of change of γ is proportional to the local slope we can see that the phase γ will spend a long time slowly creeping along when it is on

any of the shoulders of the potential profile. This corresponds to $\gamma \sim \frac{\pi}{2}$ in which case we have the largest supercurrent contribution possible. In this case $\frac{I}{I_c} - \sin\gamma \sim 0$. However, when it reaches the ledge separating adjacent shoulders, $\gamma \sim \frac{3\pi}{2}$ and $\frac{d\gamma}{d\tau}$ is maximal. In this case the supercurrent actually opposes the current bias. In order to minimize energy, the junction spends as little time here as possible. Each of these cycles corresponds to jumps of 2π of the phase across the junction. We can use the relationship $\frac{d\gamma}{d\tau} = \frac{2eV}{\hbar}$ to find the change of flux across the junction:

$$\Delta\phi = \int_0^T V(t)dt = \int_0^T \frac{\hbar}{2e}\frac{d\gamma}{dt}dt = \int_0^{2\pi} \frac{\hbar}{2e}d\gamma = \frac{h}{2e} = \phi_0.$$

Thus, in each cycle of the junction, the supercurrent oscillates between positive and negative, a voltage spike occurs for a short moment of time while the supercurrent is negative, and one quantum of flux is passed "along" the junction insulator. This makes some sense if we imagine completing the RCSJ model with a current source in a closed loop. Each 2π phase cycle corresponds to an induced voltage across the junction. Such a voltage spike will be proportional to a rate of change of the flux through Faraday's law. By passing one flux quantum either into or out of the circuit (depending on the current bias direction), we are satisfying this requirement.

Phase slips (quantum and otherwise)

Unfortunately, I know of no simple set of equations that can define the essentials of a phase slip event in analogy to the simply math that yields the two essential Josephson relations. However, we can build on our previous understanding of the JJ and it's tilted washboard potential to consider thermal- and quantum-induced phase slips in a nanowire.

Phase slip events consist of local moments in time and space where superconductivity is spontaneously destroyed. This can be attributed to either thermal or quantum fluctuations. In a nanowire these events are particularly important because the width of the wire is much less than the superconducting coherence length. These fluctuations of the superconductivity must be on the order of the coherence length because this is the minimum length over which we can define large changes in the superconductor. In a thin nanowire, the fluctuation can momentarily block the supercurrent along the wire and create a situation which causes finite dissipation. In macroscopic wires these fluctuations are negligible. For example, if we consider a superconducting wire in a real laboratory magnet, the diameter may be of order 1 mm. The coherence length ξ may be of order 100 nm. Because thermal and quantum fluctuations over a large energy Δ which is of order $1 - 10$ K are rare, the odds of several fluctuations of size ξ^3 all killing superconductivity simultaneously over the entire cross sectional area of the wire are exponentially small. We can imagine if one such blip does momentarily block a small portion of incoming supercurrent. If there are adjacent areas which are still superconducting, the supercurrent will simply go around the fluctuation and everything will be restored to usual operation once the fluctuation has died. No voltage accumulates along the wire in this process.

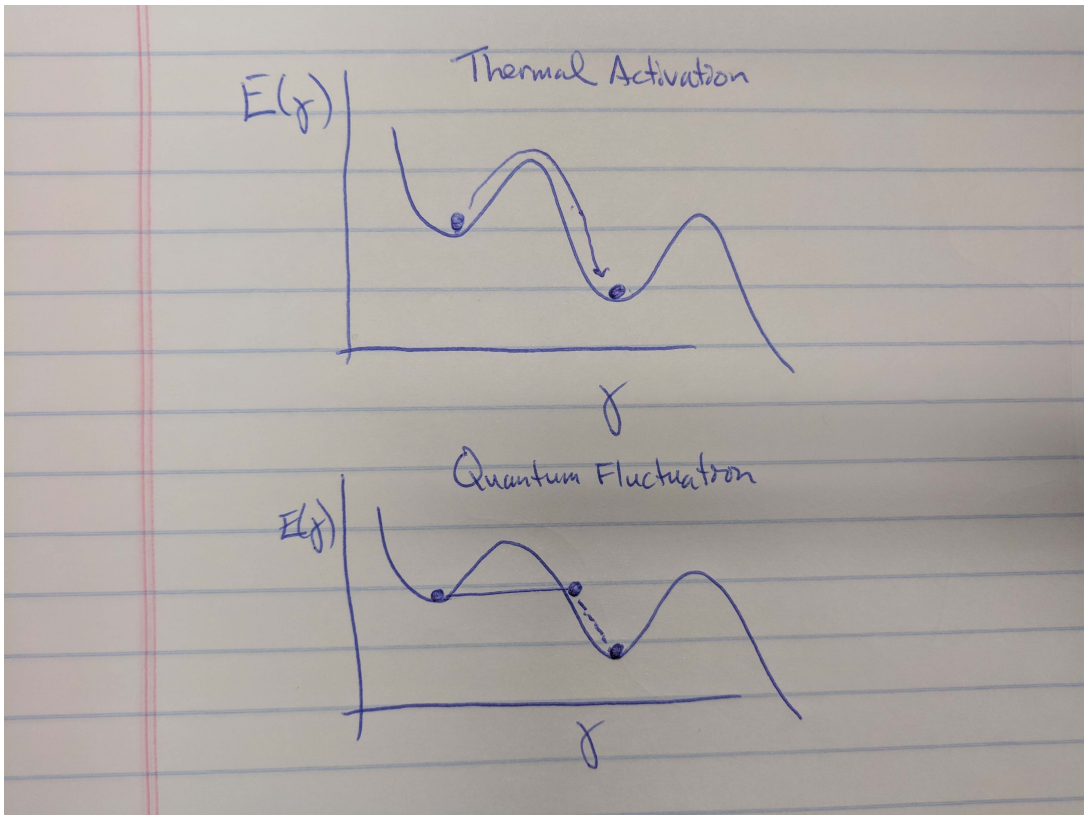

Figure 3: We can treat the spontaneous fluctuations in a superconducting nanowire in the limit of the tiled washboard model. We assume before the fluctuation we have a very large critical current I_c. Our phase is trapped, but thermal (top) or quantum (bottom) fluctuations may change our phase in jumps of 2π.

In a nanowire, because of its narrow width, all it requires is one single fluctuation to stymie the supercurrent momentarily. If a nanowire experiences such a situation in which it is momentarily blocked, we can treat the wire as if it were a JJ. Before the blockage occurs, we can imagine that the nanowire is a JJ in the limit of a vanishing tunneling barrier (i.e. it is a standard superconducting wire). We might picture this as a situation in which the critical current is extremely large and so we could draw a tilted washboard model in which our potential profile is dominated by the sinusoid term and has a very small slope as shown in Fig. 3. Using this picture, a thermal fluctuation would look like giving our phase "particle" a little kick. We could imagine that a suitably large kick could send our particle over the barrier and into the next well minimum, thus acquiring an extra phase of 2π. This would correspond to a temperature fluctuation which spontaneously gaps out the superconductor at one point in space – a thermally activated phase slip. Moreover we could also imagine treating the phase γ as a quantum object instead of a classical particle along a track. We could picture it tunneling through the free energy barrier (the adjacent hump) into the next well minimum, also acquiring a phase of 2π. This is a quantum phase slip event. The origin of this process lies in the uncertainty principle. Whenever we localize charge, it's conjugate variable γ

will experience fluctuations. As we've motivated with the previous discussion of JJs, these phase slips of 2π correspond to a factor of ϕ_0 crossing the wire. Thus, the flux is jumping with each event. Because the current bias tilts the potential, we should expect to get phase (and flux) jumps in one direction preferentially.

The previous description of thermal and quantum phase slips accounts for a large body of research on dissipation in nanowires. In particular, thermally activated phase slips can be modeled well and the experimental data on finite voltages measured below T_c match theory extremely well. Finite voltages at temperatures far below T_c are thought to be possibly explained by quantum phase slips. However, it is difficult to unambiguously attribute dissipation to quantum phase slips because at the length scales of a nanowire, other dissipative effects may play a role. For example, a mixture of granular superconducting islands separated by an insulating matrix would look like a network of JJs or may experience Coulomb blockade depending on the details of the grain size. If any location along the nanowire experiences enhanced disorder, this may also effectively kill the superconductivity over a small region. Such mechanisms are difficult to rule out with transport alone (which constitutes all previous measurement attempts).

In the previous discussion of quantum phase slips, I did not mention whether or not such a tunneling event could be coherent. In general, such a phase slip is not expected to "remember" its previous phase. An intriguing possibility arises if coherent tunneling were possible: the nanowire could be capable of existing in a superposition of two different phase winding numbers, mediated by flux quanta hopping back and forth in a coherent fashion. We could picture an analogous situation in which we have a molecule with two atomic wells which are separated by a barrier. If we populate the molecule with one electron, the coherent tunneling or hopping between the two well sites allows the electron to occupy hybrid states composed of symmetric and antisymmetric (bonding and anti- bonding) combinations of the wave functions of the two isolated wells. In an admittedly much more complicated fashion, we can picture such coherent tunneling as providing the "hopping" term between adjacent flux-number states, opening the door to interference-based quantum phenomena.

Circuit implementation

In the previous section we discussed some of the pitfalls of attempting to measure quantum phase slips in nanostructures. Namely, other dissipative effects may make interpretation of DC voltages difficult. In order to avoid this, we must perform some type of AC or time-domain measurement in which the QPS site is coupled to a circuit for readout. One way of achieving this is to close the nanowire into a loop and inductively couple it to a nearby measurement circuit. Instead of bending the nanowire itself into a loop (which might be difficult if we need to make a really long, uniform nanowire) we can instead build a circuit which consists of a nanowire segment attached to a wider section of the same superconducting material which is bent into a loop as shown in Fig. 4. First we will calculate this circuits Hamiltonian without explicitly considering the

phase-slip process. Subsequently, we will consider coherent quantum phase slips perturbatively to determine how the spectrum will change.

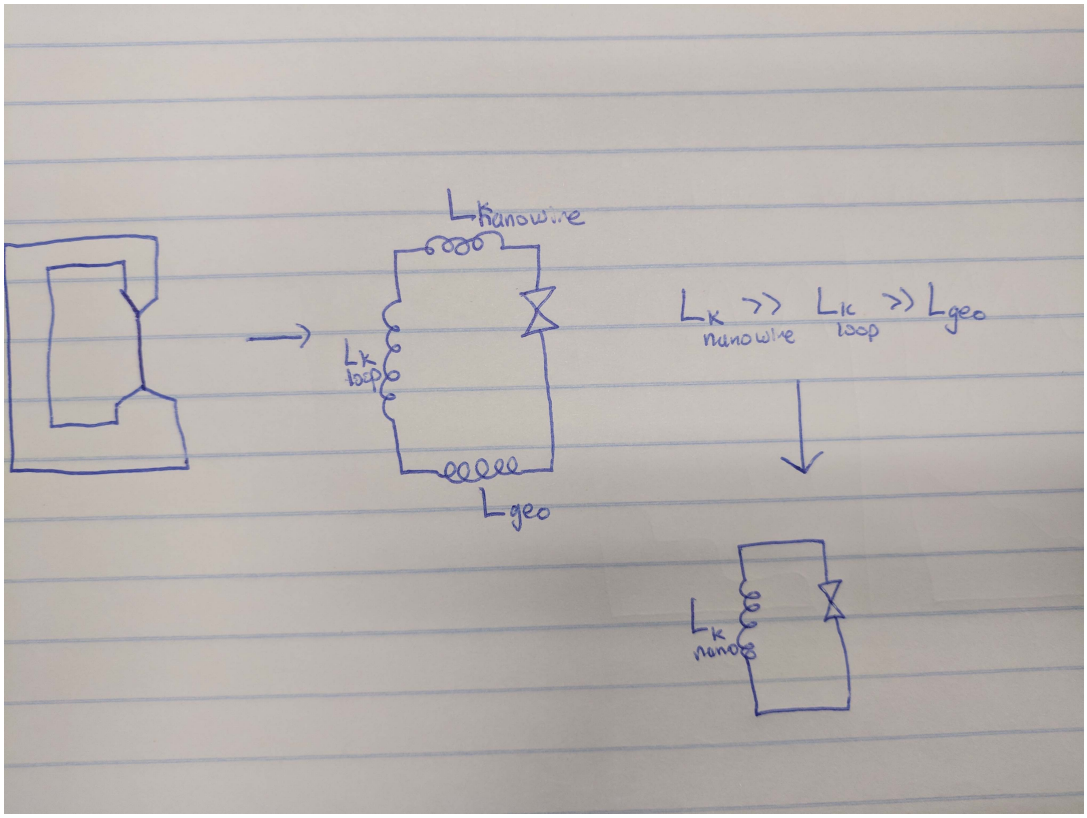

Figure 4: We can use a segment of nanowire bent into a loop (with a wider section) as an object to measure. The equivalent circuit is represented by a simple loop with a QPS site and several inductances related to both the geometry of the circuit and the kinetic inductance of the superconductor. It turns out we can neglect all but the kinetic inductance of the nanowire segment.

The kinetic energy of the circuit will simply be given by

$$T = \frac{1}{2} L I^2$$

where L is the total inductance of the loop. The most obvious source of inductance is the trivial geometric self-inductance of the circuit L_{geo}. In superconductors it turns out that there is another very important source of inductance: the kinetic inductance L_k. The kinetic inductance is a circuit impedance that arises from the inertial tendency of charge carriers to want to remain in motion. All electrons, holes, Cooper pairs etc have mass. When one sets up a steady current, these particles don't want to suddenly slow down or speed up. We can calculate this impedance for the case of the superconductor by equating the total inductive energy with the kinetic energy of the discrete charge carriers:

$$\frac{1}{2}L_k I^2 = \frac{1}{2}(2m)v^2 N$$

where $N = nAl$ is the total number of charge carriers along a given section of wire of length l and area A with carrier number density n. Using the expression $I = An(2e)v$ for the current we find:

$$L_k(An(2e)v)^2 = 2mv^2 nAl \Rightarrow L_k = \frac{ml}{2e^2 An}$$

This expression is only different for normal metals and semiconductors by numerical factors related to the mass and charge terms. This expression reveals why the kinetic inductance is only relevant for superconductors. The kinetic inductance $L_k \sim \frac{1}{n}$. Because the superfluid density of a superconductor is much lower than the total electron density of a metal, the individual speed of the charge carriers is much larger in a superconductor and hence have a much larger kinetic energy (per particle). Additionally, when we approach the small n limit of metals and semiconductors, we also begin to get appreciable resistance R which will dominate any small L_k contributions. As $R = 0$ in a superconductor, we are dominated by this kinetic inductance.

In our circuit that we have described above, we should really consider the kinetic inductance from two sources: that of the small nanowire and that from the larger, thick section of the loop. But we can see from this expression that the kinetic inductance $L_k \sim \frac{1}{A}$. So even though the number density of carriers is the same in each portion of the loop, because an identical current must run through a narrow section which allows fewer carriers, their speed within the nanowire must be much greater, leading to a much larger kinetic inductance. Thus, we will suffice to treat our circuit as a simple loop with one inductance L_k associated with the nanowire and a (coherent) QPS site which we will treat as a perturbation shortly.

We will now derive the kinetic energy of the system. Let us first note that in superconductors which form a closed loop, the flux enclosed must be an integer multiple of the flux quantum ϕ_0. This can be easily derived. Let the macroscopic wave function be defined as $\psi = \sqrt{n}e^{-i\alpha(r)}$ where n is the number density of Cooper pairs and $\alpha(r)$ is the position-dependent phase. We can calculate the current density J through:

$$\mathbf{J} = (-2e) < \psi|\mathbf{v}|\psi > .$$

In the presence of a finite vector potential $\mathbf{A}$, the kinetic momentum is given by $m\mathbf{v} = -i\hbar\nabla - 2e\mathbf{A}$. Thus we find:

$$\mathbf{J} = -\frac{2en}{m}\left(\hbar\nabla\alpha - 2e\mathbf{A}\right).$$

We can now integrate this equation around a contour deep within the superconducting loop and exploit the fact that the current density will be limited to the surface of the superconductor. Therefore $\mathbf{J} = 0$ along the contour and we find:

$$0 = \oint \mathbf{J} \cdot \mathbf{dl} = -\frac{2en}{m}\left(\hbar\Delta\alpha - 2e\phi\right)$$

where we have used the fact that $\oint \nabla\alpha = \Delta\alpha$ and $\oint \mathbf{A} \cdot \mathbf{dl} = \phi$. Defining the total phase change around the loop to be $\gamma = \Delta\alpha$ we find:

$$\phi = \frac{h}{2e}\frac{\gamma}{2\pi} = \phi_0\frac{\gamma}{2\pi}.$$

But we know that the phase must satisfy $\gamma = 2\pi n$ around the full loop in order for the wave function ψ to be single valued. Thus:

$$\phi = n\phi_0$$

Returning to our circuit implementation, let us imagine a loop with inductance given by L_k, a QPS site which we will introduce as a perturbation, and some external flux threading the loop which we can control in the laboratory given by ϕ. The conclusion of the previous derivation is that no matter what external flux we apply, the total flux (which is the sum of the external flux and the flux generated by screening currents of the superconducting loop) must equal an integer number of flux quanta. Thus, the circuit can be indexed by the number of flux quanta $n \in \mathbf{Z}$. However, despite the fact that various states labeled by n are allowed, they are not all equivalent in the energy cost. If we are required to generate enormous screening currents, this will cost us an inductive energy $T = \frac{1}{2}L_k I^2$. Because L_k is current-independent, the larger the screening current, the larger the kinetic energy cost. This neglects the work required to create the external flux of course, which we take for granted.

We can calculate the total kinetic energy as follows: first choose an index n of total flux we wish to describe. Let the external flux be normalized by the flux quantum such that $\phi_{\text{ext}} = f\phi_0$ with $f \in \mathbf{R}$ not restricted to be an integer. The total flux through the circuit must satisfy:

$$n\phi_0 = f\phi_0 + L_k I_p \Rightarrow I_p = (n-f)\frac{\phi_0}{L_k}.$$

The kinetic energy is then:

$$T = \frac{1}{2}L_k I_p^2 = \frac{\phi_0^2}{2L_k}(n-f)^2 = E_L(n-f)^2$$

where we have defined an inductive energy scale $E_L \equiv \frac{\phi_0^2}{2L_k}$. Thus, we get a series of parabolas centered around $f = n$ as depicted in Fig. 5. Note that the variable f is continuous and allows us to shift the bias point of the external flux. Thus we could plot a series of parabolas all shifted by units of ± 1 on the horizontal f-axis. What does it mean to have this series of parabolas? They make

physical sense in the following way: our flux bias f will place us closest to one of the parabolas for a particular n'. This means that the ground state consists of n' flux quanta through the loop. The physical interpretation is that the external flux brings us quite close to a particular integer n' and we only have to set up a small persistent current I_p to compensate the extra flux because $|n' - f| \leq \frac{1}{2}$. The maximum energy cost is $E_{n'} = \frac{E_L}{4}$. If we were to choose a different flux quanta n'' which is far away from the bias point $|n'' - f| \gg 1$ then the energy cost will be significant: $E_{n''} \gg E_{n'}$. This is due to the extremely large persistent current which must run through our substantial inductance: $\frac{1}{2} L_k I_{n'}^2 \leq \frac{\phi_0^2}{8L_k} \Rightarrow I_{n'} \leq \frac{\phi_0}{2L_k}$. For the n'' state we find: $I_{n''} = \frac{\phi_0}{L_k}|n'' - f| \gg I_{n'}$.

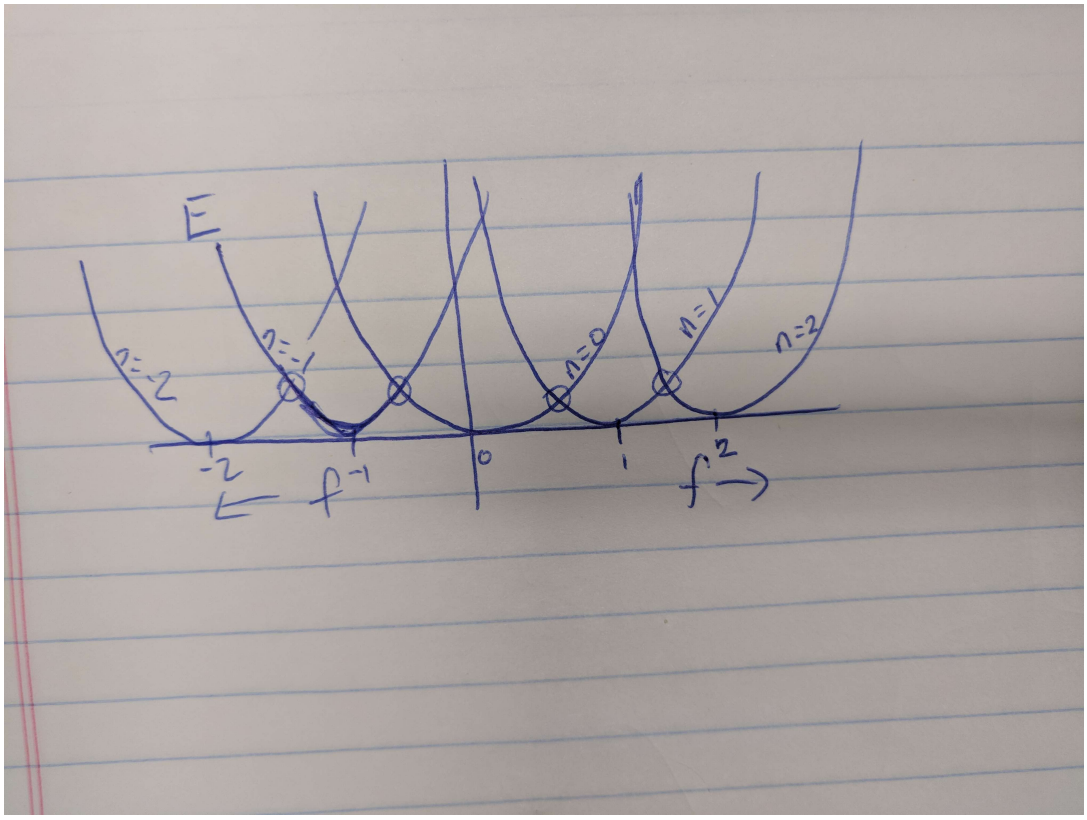

Figure 5: The kinetic energy of the circuit consists of a series of parabolas describing different numbers n of flux quantum within the loop. Depending on our external flux bias f, different parabolas may cost more or less energy. The ground state (the lowest set of lines in the figure) can be traversed by application of external field f.

One important feature of this landscape is the fact that whenever $\phi = \frac{1}{2}\phi_0$ (i.e. $f = \frac{1}{2}$), we have a degeneracy between two adjacent flux states $n, n+1$, depicted with circles in Fig. 5. This makes physical sense: if we perfectly bias a half-integer of excess flux through the loop we can either run a half-flux portion of current one direction (say clockwise) to add the missing $\frac{1}{2}\phi_0$ or we can run the same magnitude current in the counterclockwise direction to subtract the excess flux. Each option costs us the same energy.

Let us know introduce the notion of coherent QPS with an amplitude E_S. We will only focus

on phase slips of $\pm\phi_0$ because we are only concerned with the low energy physics. Because this interaction couples $n \leftrightarrow n+1$ states (coherently), the degeneracies at the locations $f = \frac{1}{2}$ mod 1 will be lifted. The ability to shuttle one flux quantum across the nanowire means that we no longer have definite amounts of flux quanta within the loop: the circuit can now exist in a superposition of counterrotating persistent currents. The Hamiltonian can now be cast in the basis of $|n>$ as:

$$H = E_L(n-f)^2|n><n| - \frac{E_S}{2}\sum_n(|n+1><n| + |n><n+1|)$$

In our diagram of parabolas we will gap out the degeneracies to create avoided crossings due to the interaction E_S as seen in Fig. 6. We can zoom in on this small region of phase space and consider the low energy physics. It is approximately a two-level system and we can diagonalize in the local subspace containing only the relevant states: $n, n+1$. We find:

$$H = \begin{pmatrix} E_n & -E_S/2 \\ -E_S/2 & E_{n+1} \end{pmatrix}.$$

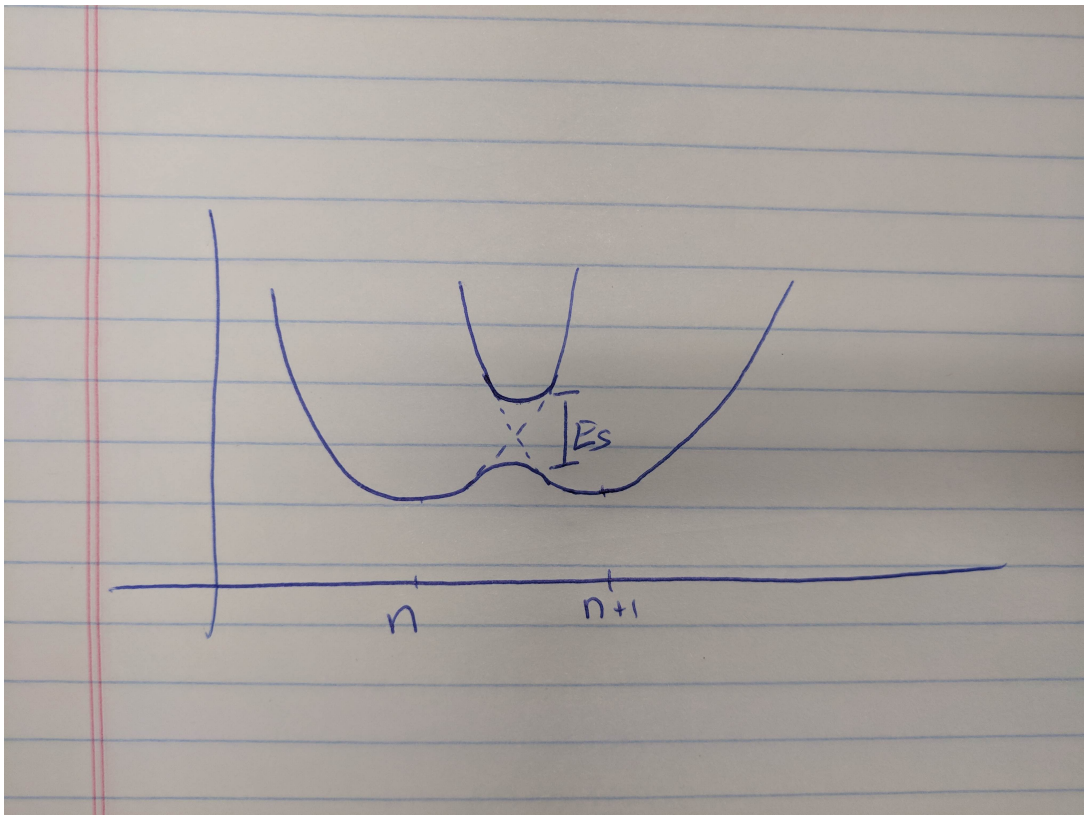

Figure 6: If we examine the crossing of the n and $n+1$ branches of the Hamiltonian we create an avoided crossing if an interaction E_S can couple the two states coherently.

We can simplify by subtracting E_n along the identity and computing:

$$E_{n+1} - E_n = E_L \left((n+1-f)^2 - (n-f)^2 \right) = E_L \left(2\left(n-f\right) + 1 \right).$$

Since we are concerned with small deviations around the degeneracy we can set $f = n + \frac{1}{2} + \delta$ to find

$$E_{n+1} - E_n = -2E_L\delta.$$

Solving for the spectrum we get

$$E_{\pm} = -E_L\delta \pm \frac{1}{2}\sqrt{(2E_L\delta)^2 + E_S^2} \Rightarrow \Delta E_{\pm} = \sqrt{(2E_L\delta)^2 + E_S^2}.$$

This is an important equation - if we have coherent QPS, then we should expect transitions between the ground and excited states at this energy $\Delta_{\pm}$ which we can tune by changing our external flux (here indicated by δ).

Did we ever use the fact that this process is coherent? Yes - by allowing the interaction energy E_S to couple two states in a deterministic way via the Hamiltonian, we are implicitly assuming that the phase slip process is coherent. If it were not coherent, we would not have an avoided crossing. If we biased close to the degeneracy point, the circuit would become metastable and may transition from $n \leftrightarrow n+1$ stochastically due to quantum fluctuations. But the circuit would never exist in a stable superposition of two flux states. We could perhaps describe the circuit with a density matrix representing the n-state 50% of the time and the $n+1$ state 50% of the time. Importantly, this representation would not produce any interference effect.

Optional: Duality to the Cooper pair box

A brief aside: the Hamiltonian given above looks very similar to a completely different circuit. In fact if we exploit our duality transform and swap capacitors for inductors, JJs for QPS sites, etc we would end up with a circuit called a Cooper pair box shown in Fig. 7. It consists of an island of superconductor which is coupled on one end to a capacitor and the other end with a JJ connected to a charge reservoir. If the island has a small capacitance, then the energy to add charge to the island can be substantial due to the fact that $E_C = \frac{(2e)^2}{2C}$ can be arbitrarily large for small enough C (the total capacitance of the island). This charging energy is similar to the inductive energy $\frac{\phi_0^2}{2L_K}$. The JJ will couple different charging states of the island in the same way that the phase slip site couples different flux states. We could write a similar Hamiltonian of the form:

$$H = E_C(n-f)^2|n><n| - \frac{E_J}{2}\sum_n \left(|n+1><n| + |n><n+1|\right)$$

where n now represents the number of Cooper pairs on the island and f the continuous charge induced on island by the gate normalized by the Cooper pair charge: $VC_{\text{gate}} = f(2e)$. In fact, if

we exploit the fact that n, γ are conjugate operators we can compute:

$$\begin{aligned}\sum_n |n><n+1| &= \sum_n \int_0^{2\pi} d\gamma' \int_0^{2\pi} d\gamma e^{-i(\gamma-\gamma')n} e^{i\gamma'} |\gamma><\gamma'| \\ &= \int_0^{2\pi} d\gamma' \int_0^{2\pi} d\gamma \delta(\gamma-\gamma') e^{i\gamma'} |\gamma><\gamma'| \\ &= \int_0^{2\pi} d\gamma e^{i\gamma} |\gamma><\gamma|.\end{aligned}$$

Thus,

$$\frac{E_J}{2} \sum_n (|n+1><n| + |n><n+1|) = E_J \cos\gamma |\gamma><\gamma|$$

where we are implicitly integrating over γ. This is a striking example of the duality between the JJ and the QPS site.

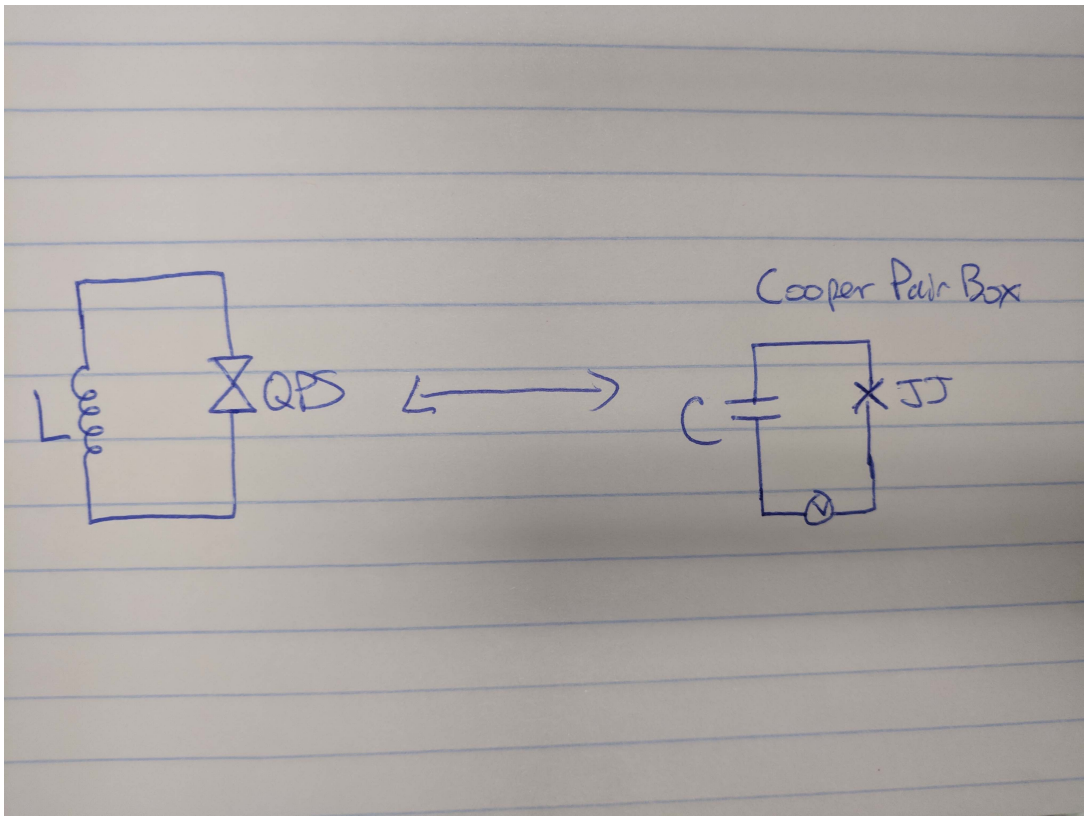

Figure 7: The QPS site embedded in a loop (left) can be mapped to the Cooper pair box (right) through a duality transform. The Hamiltonians take the same form in the number basis-$|n>$.

Measurement and experimental details in first reference

We've discussed the necessity of measuring CQPS through some non-transport means and we've even worked out the details of a potential circuit implementation. In order to map out the Hamiltonian of this system, we need to use a spectroscopic technique. The one which has been used by the authors is to couple the CQPS site (which is embedded into a loop) to a coplanar waveguide as seen in Fig. 8. They have chosen to use InOx as the superconducting material of choice because it is expected to have extremely large order parameter fluctuations. This is due to the fact that the material is highly disordered and there is evidence that close to the disorder-induced superconductor-insulator transition Cooper pairs become localized (while still remaining paired) before crossing through the phase boundary. In other words, the ideal material is one in which Cooper pairs can be localized without destroying superconductivity. The localization of Cooper pairs will cause large fluctuations in the phase of the wire due to their conjugate nature.

We can picture our total system as consisting of the CQPS loop and the waveguide as two coupled entities. The waveguide is characterized by its length L along with the capacitance c and inductance l per unit length. Waves traveling in this approximately lossless waveguide have a velocity given by $v = 1/\sqrt{lc}$. Because the impedance of the ends of the cavity are large, we can treat the waveguide as a cavity. The fundamental mode of this cavity occurs when a half-wavelength of the mode is equal to the length of the cavity: $L = \frac{\lambda}{2}$. This yields the relationship $\omega_0 = \frac{\pi v}{L}$. Higher harmonics are given by $\omega_n = (n+1)\omega_0$ as seen in panel (a) of Fig. 9. It turns out that we can treat the waveguide as an LC oscillator (a parallel L and C circuit) for each independent mode ω_n. If we consider the Hamiltonian of such a mode: $H_n = \frac{Q^2}{2C} + \frac{\phi^2}{2L}$. Noting that Q and ϕ are canonically conjugate variables, we can exactly map this Hamiltonian onto the harmonic oscillator Hamiltonian. We can therefore imagine our coplanar waveguide as a platform which can be "loaded up" with photons of frequency ω_n for any harmonic mode n.

Let's recap what we have: we have our CQPS site loop which is inductively coupled to a coplanar waveguide. The strength of the coupling is proportional to the magnitude of the current in the waveguide at the halfway point. It turns out that resonant frequencies ω_n with n odd have a node at $L/2$. Therefore, the loop and waveguide only experience coupling for $n = 0, 2, 4, \ldots$ Thus, we have a two-level system of a given resonance frequency Ω along with a harmonic oscillator of frequencies ω_n. We can imagine interacting in two different limits. If we look at the case in which $\omega_n \sim \Omega$ for some even n, then we are in a strongly coupled regime in which photons can be exchanged coherently between the CQPS circuit and the waveguide. If we can measure the transmission of photons through the waveguide, we will note that the transmission will be strongly reduced whenever the CQPS is resonant due to the fact that photons will spend some of their time inside the CQPS circuit instead of propagating through the transmission line. Panel (b) in Fig. 9 shows the measured transmission and phase as a function of external magnetic field while operating at the fourth harmonic ω_4. We can see that the transmission dips twice (due to the fact that $\hbar\omega_4 = \Delta E_\pm = \sqrt{(2E_L\delta)^2 + E_S^2}$ will have two solutions for $\pm\delta$) and is periodic with

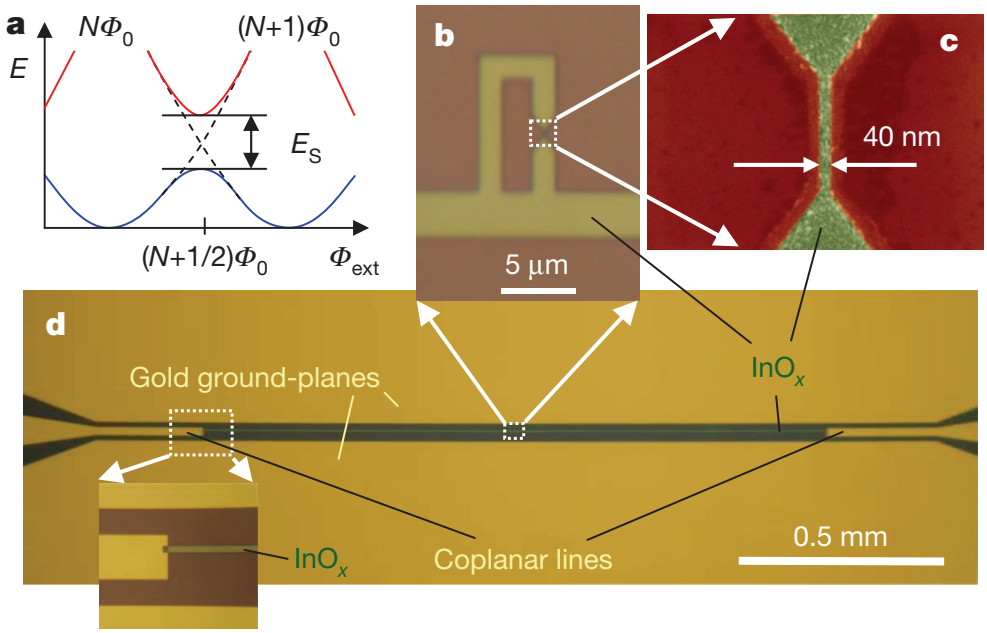

Figure 8: **Figure 1 from the first reference.** (a) The avoided crossing of the CQPS site due to phase slip amplitude E_S. (b) Zoom-in of the superconducting loop from panel (d). (c) Zoom-in of the nanowire segment in panel (b). (d) Image of the coplanar waveguide and coupled circuit.

magnetic field. The periodicity in magnetic field can be related to an area via $\phi_0 = A\Delta B$. We find that $A = 32\,\mu\text{m}^2$ which agrees well with the lithographic area of the loop.

This tells us quite a bit, but we would like to map out the full excitation spectrum $\Delta E_\pm = \sqrt{(2E_L\delta)^2 + E_S^2}$. In order to achieve this, the experimenters use what's known as a two-tone measurement. The idea is related but distinct from panel (b) of Fig. 9. The logic is as follows: the coplanar waveguide and two-level system (the loop) are a completely coupled object. The physics of one influences the physics of the other. It is obvious in the resonant case when we drive the waveguide with a frequency $\omega \sim \Omega$ (the Rabi limit) because the loop and waveguide are able to directly exchange photons back and forth. However, even if we drive the resonator with a frequency ω such that $|\omega - \Omega| \gg g$ where g is the coupling strength (here it is proportional to the mutual inductance of the loop and planar waveguide as well as the magnitude of the current), the characteristics of the resonator will still be influenced by the presence of the loop, and specifically, whether or not the loop is in its ground state. This is the so-called dispersive limit. The details can be solved by taking the Jaynes-Cummings Hamiltonian (describing the cavity-photon system) and expanding to second order in powers of $\frac{g}{|\omega-\Omega|}$. The relevant point for our measurement is that when driven off-resonance, the waveguide will experience a shift in its resonant frequency given by $\pm\frac{g^2}{|\omega-\Omega|}$ where the $\pm$ correspond to the excited (ground) state of the QPS loop. If we measure using the fourth harmonic as done in the reference, the shift is given by $\pm\frac{g^2}{|\omega_4-\Omega|}$. This allows us to monitor properties of the loop even when using a driving frequency that is far from resonance.

The second tone in a two-tone measurement is used to modulate the state of the loop, which

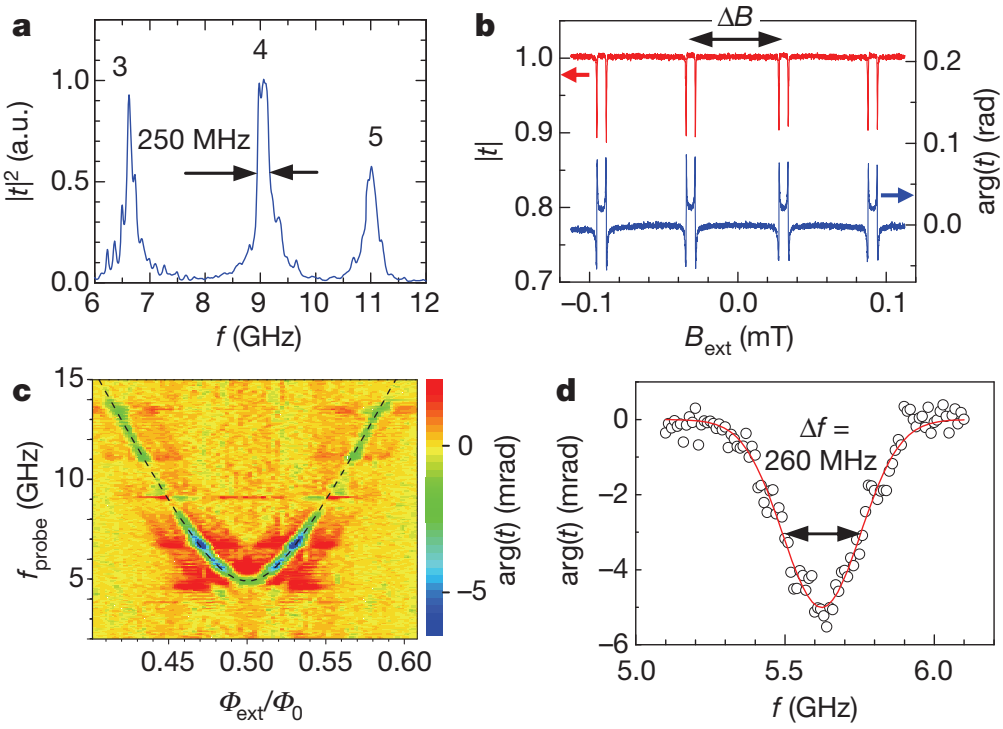

Figure 9: **Figure 2 from the first reference.** (a) Transmission through the resonator as a function of frequency. (b) Transmission and phase of the the signal operating at ω_4. As the magnetic field is changed, we are pushed left and right through Fig. 5. Whenever the energy gap between ground and first excited state equals $\hbar\omega_4$ we experience a dip in transmission due to the strong coupling (Rabi limit). (c) Two tone measurement in which one small "probe" tone close to ω_4 is applied to the resonator. At the same time, an excitation probe of variable frequency is scanned. Whenever this larger excitation frequency is equal to the energy gap, the resonant frequency of the transmission line is shifted slightly due to the resonator–loop coupling. . This causes a change in the phase of the signal leaving the transmission line. (d) Broadening of the detected signal.

in turn affects the size of the shift. If we apply a second tone which is far away from the resonance condition Ω, then the loop simply stays in the ground state the entire time and the frequency shift we measure is $-\frac{g^2}{\omega_4-\Omega}$. If we approach resonance, the loop will spend more of its time in the excited state and the frequency shift will increase in magnitude towards $+\frac{g^2}{\omega_4-\Omega}$. So our frequency shift (inferred by either the transmission or phase of the output of the cavity) will be a measure of which energies drive transitions in our two-level system. In Fig. 9 panel (c) we can see the results of such a scheme. The phase of the output signal is tracked as a function of both external field (i.e. δ) and excitation frequency which here is labeled f_{probe} (this is different from my language in which I call this f_{exc}). We can see that $\Delta E_{\pm} = \sqrt{(2E_L\delta)^2 + E_S^2}$ has been mapped out and can be used to extract the value of $E_S = 4.9\,\text{GHz}$.

In order to map out the full spectrum at higher energies, the authors use higher harmonic excitations. In this scheme, the authors look for multi-photon resonances which correspond to $\omega = \omega_{\text{exc}} + n\omega_4$. The $n = 0$ case was presented in Fig. 9. We can imagine instead of absorbing

one microwave photon ω_{exc}, the loop can also absorb an integer number of the cavity photons ω_4, effectively extending the microwave coupling excitation frequency. These processes are less frequent but allow the experimenters to access energies beyond the bandwidth of their apparatus. In Fig. 10 we can see the full spectrum mapped out to about 80 GHz. The extremely linear behavior at large δ indicates that the inductance (proportional to $\Delta E/B$ at large δ) is extremely linear. This establishes that the physics being measured is not due to a rogue Josephson junction which would have a very nonlinear inductance. The dotted blue line is the expected behavior of a rogue Josephson junction given the material and geometric values of the nanowire segment.

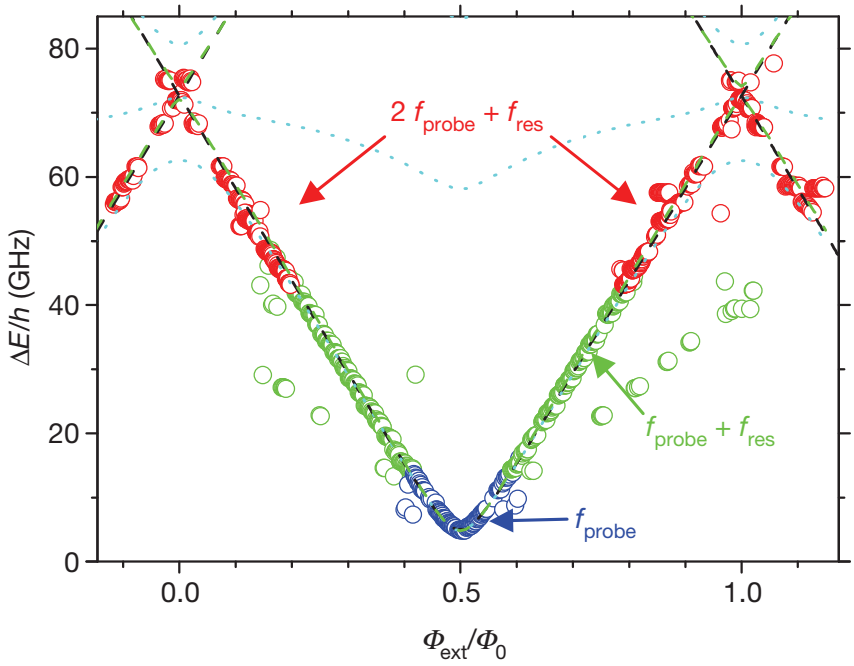

Figure 10: **Figure 3 from the first reference.** Higher harmonic excitations (due to absorption of both ω_{exc} as well as n photons of ω_4) allow access to higher experimental energies. The Hamiltonian of the system is mapped out as a function of field and energy. Linear behavior at large δ is observed, indicating an extremely linear inductance. The dotted blue line is a simulation of the expected behavior were there to be a rogue Josephson junction. Its highly nonlinear inductance shows dramatically different behavior.

In summary, the first reference demonstrates using a microwave impedance spectroscopy technique that phase slips in a superconducting nanowire can be coherent. The coupling strength between the cavity and loop is directly proportional to E_S, the amplitude of the phase slip interaction strength. Furthermore, they were able to map out the excitation spectrum of the ground and first excited state, confirming the expected dependence on energy and magnetic field. By avoiding a DC transport technique, the authors have sidestepped the issue of interpreting dissipative phenomena. It is still possible that some sort of rogue Josephson junction could exist within the nanowire, but the expected behavior would look quite different as shown in Fig. 10. Furthermore, they observe similar behavior with phase slip amplitudes in the neighborhood of $4 - 9$ GHz in

multiple devices, ruling out the likelihood of a spurious two-level system. The matter of whether this is a *coherent* phase slip process has already been implicitly assumed. The only way the two-level system could be created in the first place is if there is a coherent interaction that connects the n and $n+1$ branches of the Hamiltonian and the coupling $g \sim E_S$, enabling the technique in the first place. Thus, the reference puts coherent quantum phase slips on firm footing.

Brief commentary on second reference

The motivation of the second reference is to use this newfound object (the coherent quantum phase slip site) as an analogy of the Josephson junction. Just as a JJ is the building block for the SQUID, we can imagine building a similar dual object from CQPS sites. We can simply flip all of the elements of a SQUID to their dual components. Instead of combining two **JJs** in **parallel** in a **loop** with a threaded magnetic field which can modulate the **flux** through the loop as in a traditional DC SQUID, we can combine two **QPS sites** in **series** with an **island** separating them with an external voltage which can modulate the number of **Cooper pairs** on the island. The idea here is that instead of a Cooper pair traveling around a loop, the flux quanta can circle the island by entering and exiting through the two QPS sites. This basic scheme is shown in panels (a) and (b) in Fig. 11.

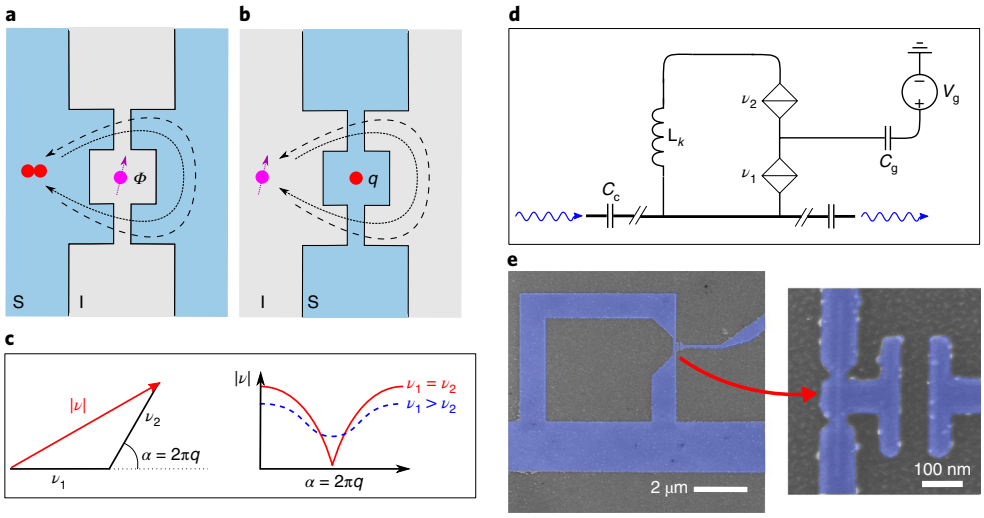

Figure 11: **Figure 1 from the second reference.** (a) Traditional DC SQUID (b) CQUID (c) The vector sum of the two phase slip amplitudes and associated dependence on island charge (d) Measurements schematic (e) Images of the NbN film

As a reminder, the JJ is described by a condition on its current given by $I = I_c \sin\gamma$. Because the JJ is dual to the QPS site, we can write down an analogous equation $V = V_c \sin(2\pi n)$ where n is the number of Cooper pairs flowing through the nanowire segment. V_c is the critical voltage which is given by $\frac{2\pi E_S}{2e}$. If we note that the current running through the QPS site is given by

$I = 2e\dot{n}$ then we can find the potential energy of the QPS:

$$E = \int_0^t IVdt = \int_0^t \frac{2\pi E_S}{2e}\sin(2\pi n)2e\frac{dn}{dt}dt = 2\pi E_S\int_0^n \sin(2\pi n)dn = E_S(1-\cos(2\pi n))$$

We can neglect the constant term. If we now consider two series QPS sites with the same amplitude E_S, then the total potential energy is given by

$$E = E_1 + E_2 = -E_S(\cos(2\pi n_1) + \cos(2\pi n_2)) = -2E_S\cos(\pi(n_1+n_2))\cos(\pi(n_1-n_2)).$$

If we imagine capacitively coupling the central island between the two junctions to a voltage source V_g then conservation of charge on the island yields the relation $n_1 - n_2 = \frac{C_g V_g}{2e}$. Therefore we may rewrite the previous equation:

$$E = -2E_S\cos\left(\frac{\pi C_g V_g}{2e}\right)\cos(2\pi n)$$

where $n = \frac{n_1+n_2}{2}$. Thus, by tuning the gate voltage (the induced charge on the island) we can modulate the interference of the two junctions in much the same way that a flux bias modulates the interference of two JJs in a SQUID. If we have two QPS sites with different E_S then the previous equation will not hold exactly. We will find that the potential energy scales as -$\left|E_{S1} + E_{S2}e^{2\pi C_g V_g/2e}\right|$.

In this experiment, the two QPS sites are also embedded into a loop and coupled to a coplanar waveguide in much the same way as the previous reference. Thus, the data is easy enough to interpret in light of our previous analysis. The kinetic energy of the loop is still given by the inductive term $T = E_L(n-f)^2$ where $E_L = \frac{\phi_0^2}{2L_k}$ where now the kinetic inductance L_k consists of contributions from both series junctions. The interaction term, instead of looking like $-E_S$ will include the interference effect of both junctions (which may in general have different phase slip amplitudes). Thus, we find that the splitting between the ground and excited state will look like

$$\Delta E_\pm = \sqrt{(2E_L\delta)^2 + h^2\left|\nu_1 + \nu_2 e^{i2\pi q}\right|^2}$$

where we are now using $h\nu_i = E_{Si}$ and $q = \frac{C_g V_g}{2e}$.

The authors of reference 2 have performed the same microwave impedance spectroscopy and the data is shown in Fig. 12. In this study, they use the material NbN for similar reasons to the choice of InOx in the first reference (it can be fabricated so that it is close to its superconductor-insulator transition which yields a large rate of order parameter fluctuations). If we focus first on panels (a,b) we will see two-tone microwave measurements that look somewhat familiar to the previous reference, except we now have two branches displaced by a few GHz. The two panels are taken as a function of applied flux bias at two distinct charge states of the central island. We expect to only have one parabola, but we see two. What explains this? Well, it turns out that in addition to pure Cooper pairs traveling through the island, we also can have single electron quasiparticles. These single electrons affect the phase through sending $q \to q + \frac{1}{2}$ which causes

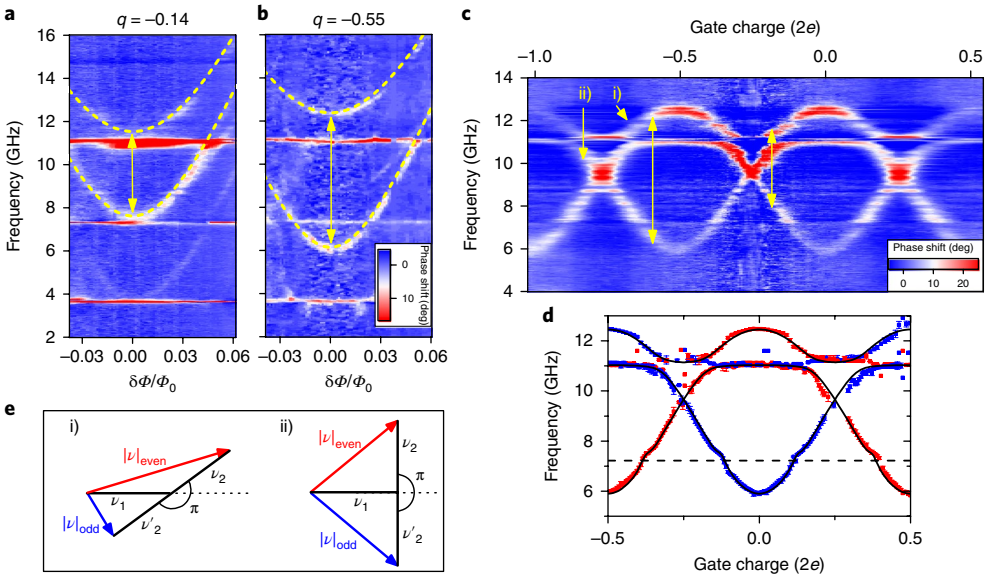

Figure 12: **Figure 2 from the second reference.** (a,b) Two-tone spectroscopy of the device for two different fixed gate voltages as a function of applied flux bias (c) Two-tone spectroscopy of the device at zero applied flux bias and variable gate charge (d) Extracted transition energies from both the odd and even parity branches (e) Reconstruction of the phase slip vectors for the points in panel (c)

$\sqrt{(2E_L\delta)^2 + h^2\left|\nu_1 + \nu_2 e^{i2\pi q}\right|^2} \rightarrow \sqrt{(2E_L\delta)^2 + h^2\left|\nu_1 - \nu_2 e^{i2\pi q}\right|^2}$. In other words, depending on the parity of the charge state of the island (even or odd), we will find two different energy splittings of the ground and first excited state. The authors postulate that quasiparticle fluctuations occur on timescales as short as 2 ns which is much shorter than their measurement timescale. Thus, in one measurement, they observe both party states with equal amplitudes. This explains the presence of a second parabola at a different energy in panels (a,b). If we look at panel (c), this picture is further substantiated. The two distinct sinusoids are offset by exactly one half of a Cooper pair period on the gate. Note that the horizontal features that intersect the sinusoids are distortions from the resonance mode of the waveguide and are unrelated to the physics we are discussing. In panel (d) they have extracted the transition frequencies for both branches and they were able to reconstruct the phasors shown in panel (e) from the labeled points in panel (c).

In Fig. 13 we see additional evidence to support this picture. Panel (a) simply looks at one of the parity branches and calculates the difference in the transition energy at $q = 0$ and $q = 1$ as a function of applied bias. In other words, we are measuring

$$\sqrt{(2E_L\delta)^2 + h^2(\nu_1 + \nu_2)^2} - \sqrt{(2E_L\delta)^2 + h^2(\nu_1 - \nu_2)^2}$$

while varying δ. We can see that the data is well fit by theory for the two values of $\nu_1 = 9.2\,\text{GHz}$ and $\nu_2 = 3.3\,\text{GHz}$. Panel (b) shows the expected deviation from perfect sinusoidal behavior (which

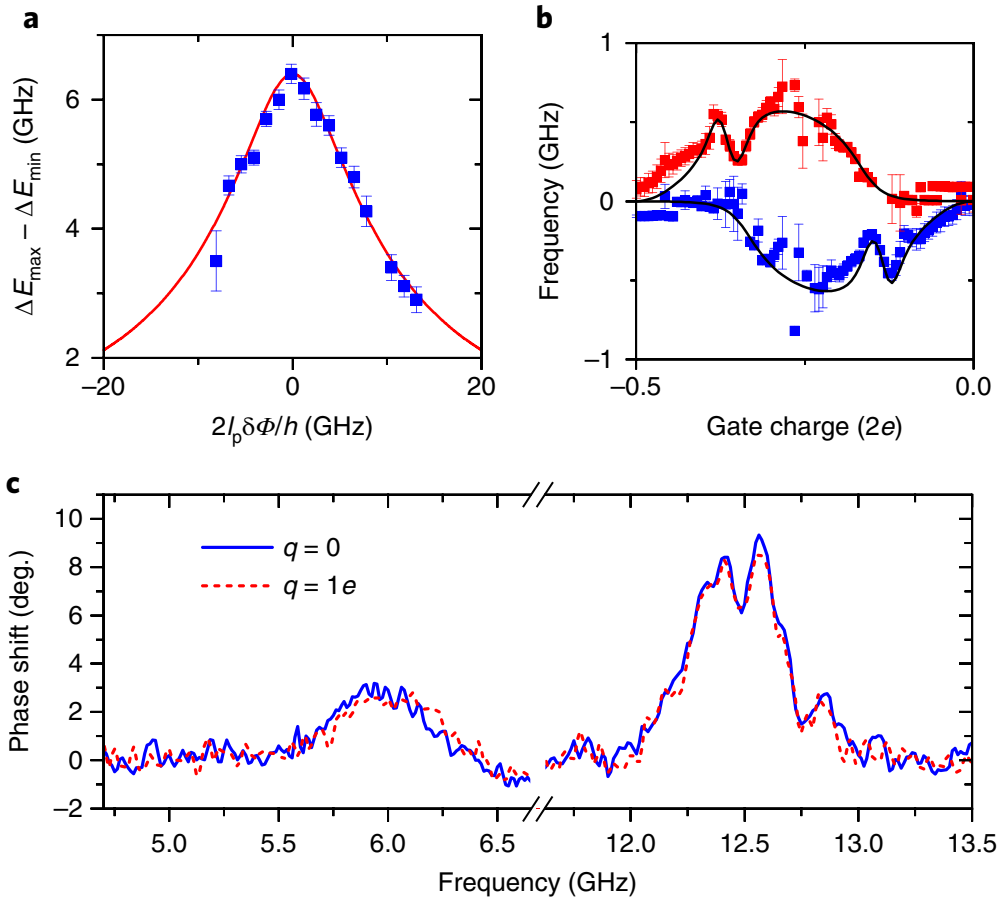

Figure 13: **Figure 3 from the second reference.** (a) Different in the transition energy when maximally and minimally separated energy levels as a function of q. The maximum separation occurs at $q = 0$ and minimum at $1e$. It is seen to decrease as expected based on our formula for $\Delta_{\pm}$. (b) Deviation of the two parity branches from pure sinusoid functions $E_S(q)$. The data is well fit to the curve which takes into account the coupling of the signal to the resonance mode of the cavity (the sharp kink). (c) Traces of each parity branch showing equal spectral weight at each parity value. The difference in height of the two branches is due to changes in coupling strength at different energies.

would be seen only for $|\nu_1| = |\nu_2|$) as a function of induced gate charge. The data is also well fit to their model, which takes into account the coupling of the signal to the resonant modes of the cavity (the sharp kink). Finally, in panel (c) the authors show that both parity branches have the same spectral weight. The difference in the peak height of the lower and upper transition energies simply arises from the different coupling strengths of the waveguide at different energies. Both branches have near identical intensity, substantiating the claim that the origin of the two branches is parity non-conserving fluctuations of the charge on the island.